

Nanoscale

Accepted Manuscript



This is an *Accepted Manuscript*, which has been through the Royal Society of Chemistry peer review process and has been accepted for publication.

Accepted Manuscripts are published online shortly after acceptance, before technical editing, formatting and proof reading. Using this free service, authors can make their results available to the community, in citable form, before we publish the edited article. We will replace this *Accepted Manuscript* with the edited and formatted *Advance Article* as soon as it is available.

You can find more information about *Accepted Manuscripts* in the [Information for Authors](#).

Please note that technical editing may introduce minor changes to the text and/or graphics, which may alter content. The journal's standard [Terms & Conditions](#) and the [Ethical guidelines](#) still apply. In no event shall the Royal Society of Chemistry be held responsible for any errors or omissions in this *Accepted Manuscript* or any consequences arising from the use of any information it contains.

Cite this: DOI: 10.1039/c0xx00000x

www.rsc.org/xxxxxx

MINIREVIEW

Biomimicry at the nanoscale: Current research and perspectives of two-photon polymerization

Attilio Marino^{*a,b}, Carlo Filippeschi^a, Virgilio Mattoli^a, Barbara Mazzolai^a and Gianni Ciofani^{*a}

Received (in XXX, XXX) Xth XXXXXXXXXX 20XX, Accepted Xth XXXXXXXXXX 20XX

DOI: 10.1039/b000000x

Abstract

Living systems such as cells and tissues are extremely sensitive to their surrounding physico-chemical microenvironment. In the field of regenerative medicine and tissue engineering, the maintenance of culture conditions suitable for the formation of proliferation niches, for the self-renewal maintenance of stem cells, or for the promotion of a particular differentiation fate is an important issue that has been addressed by using different strategies. A number of investigations suggests that a particular cell behavior can be *in vitro* resembled by mimicking the corresponding *in vivo* conditions. In this context, several biomimetic environments have been designed in order to control cell phenotypes and functions. In this review, we will analyze the most recent examples of control of the *in vitro* physical micro/nano-environment by exploiting an innovative technique of high resolution 3D photolithography, the two-photon polymerization (2pp). The biomedical applications of this versatile and disruptive computer assisted design/manufacturing technology are very wide, and range from the fabrication of biomimetic and nanostructured scaffolds for tissue engineering and regenerative medicine, to the microfabrication of biomedical devices, like ossicular replacement prosthesis and microneedles.

Introduction: Biomimicry from macro to nano

The biomimicry of an *in vivo* physiological environment has been achieved in the biomedical research at different scales, depending on the specific necessity of the application and as a consequence of the limitation of the technology adopted, in terms of resolution and fabrication times.¹⁻³ Living cells have been proven to be sensitive to the variation of several chemo-physical features, including surface roughness^{4,5} and fractal dimension^{6,7} in the range from nano to micrometers, variation of the substrate Young's modulus (E)⁸ ranging from kPa to GPa,⁹ changes in surface charge¹⁰ and wettability,¹¹ *etc.* In particular, concerning the substrate E , interesting investigations underlined as different cell types preferably adhere and grow on substrates characterized by an E similar to that of the *in vivo* environment.⁹ As an example, it is well known as neuronal, muscle and bone tissues are characterized by rather different E (in the order of GPa in the case of bone and KPa for muscle and neural tissue), and, therefore, neuronal cells preferably grow on soft substrates,^{12,13} bone cells on hard substrates,¹⁴ and muscle cells on scaffolds characterized by intermediate E values.¹⁵ Moreover, the control of the scaffolds roughness and porosity is known to be of fundamental importance in tissue engineering, and several works deeply investigated these phenomena.¹⁶ Furthermore, since natural surfaces are characterized by non-deterministic features organized over multiple scale ranges, new disordered¹⁷ and self-affine topographies were recently obtained and attracted the interest

of the scientific community: in order to mimic *in vitro* the hierarchical organization of the extracellular microenvironment, fractal substrates have been prepared through different approaches, such as electrochemical etching,⁶ traditional microfabrication methods,¹⁸ and direct laser writing.⁷ Among the different available fabrication techniques, two-photon polymerization is a photolithographic method which allows the 3D direct laser writing of different resists to be obtained, through the mechanism of two-photon absorption.¹⁹ Briefly, the simultaneous absorption of two photons (usually in the near infrared region, but not necessarily²⁰) allows for the cross-linking of a dedicated resist²¹ or of other suitable materials,²² having as a consequence the local polymerization in the so called "polymerization voxel".²³ Obviously, the 2pp resolution is given by the voxel size, which can be maintained even below 100 nm.²⁴ Owing to the transparency of the 2pp resists at the wavelengths exploited for the writing, just the region where the laser is focused and, therefore, where the two photons are simultaneously absorbed, is polymerized, thus allowing for a real 3D manufacturing. This advantage has enabled the fabrication of high-resolution 3D biomimetic structures, such as bio-inspired artificial blood vessels,²⁵ trabeculae-like scaffolds,²⁶ filamentous substrates for cardiac tissue,²⁷ *etc.*, that could not have been obtained by means of traditional photolithography approaches. Taking advantage of these 3D biomimetic structures, it was possible not only to control cell adhesion, shape and function,²⁶ but also to *in vitro* recapitulate human disease models, which can be used for high-

Cite this: DOI: 10.1039/c0xx00000x

www.rsc.org/xxxxxx

MINIREVIEW

throughput drug screening and for the investigations of pathological mechanisms.²⁷ Furthermore, the high resolution of this technique jointly to the speed of the laser writing allows the obtainment of structures characterized by a size of cm/mm owing a resolution of $\mu\text{m}/\text{nm}$,²⁸ *i.e.*, the resolution of those topographical cues to which cells are more sensitive.²⁹ The combination of high resolution and writing speed make 2pp a disruptive technology in several fields where a quick and precise micro/nano-fabrication approach represents a key issue to be addressed.

In this review, we will report on the recent innovations in 2pp that enabled an actual "biomimicry" at the nanoscale, focusing on the most important achievements concerning 2pp photoresists, on the important biological investigations carried out by exploiting 2pp structures, and, finally, on the most exciting advanced applications of 2pp in the field of tissue engineering and regenerative medicine.

Materials for 2pp: New insights

The variety of different materials available for 2pp are characterized by a wide range of properties, like different biodegradability rates, elasticity, biocompatibility, porosity and cell adhesiveness, thus enabling their exploitation for a number of different applications. For example, biodegradable photoresists such as hydrogels can mimic the presence of the extracellular matrix (ECM),³⁰ and can constitute an ideal scaffold for cell transplantation and drug delivery purposes.³¹ Different investigations have been in fact demonstrated the possibility to encapsulate cells inside the polymerizing resist,³² such as in the case of human dermal fibroblasts embedded in collagenase-sensitive poly(ethyleneglycol) hydrogels.³³ Some resists have been exploited in the biophysical investigation of the cell force measurement: as an example, Ormocomp® elastic beams have been fabricated for the measurement of cardiomyocyte contraction forces³⁴ (this work will be deeply discussed in the next section). Several other examples can be found in the literature addressing the strict correlation resist/application, and in particular the reader is referred to reviews that have already deeply discussed the characteristics of different materials that can be used in 2pp.^{30,35,36} For this reason, here we will mainly focus on the most recent approaches, that seem to be directed toward the combination of different materials to confer peculiar properties to the 3D structures.

Klein *et al.* proposed the first example of two-component scaffold prepared through 2pp. In particular, one of the used polymer (poly(ethyleneglycol) diacrylate with 4.8% of the cross-linking agent pentaerythritol tetraacrylate) is cell repellent, and was exploited for the 3D frameworks fabrication; the other photoresist (Ormocomp®) promotes instead cell adhesion, and was cured in a following step on particular sites of the frameworks. It was demonstrated as cells cultured on

these scaffolds specifically form cell-adhesion sites just on the Ormocomp® functionalized regions of the structure, so achieving a complete control of the cell adhesion and shape in a 3D environment.³⁷

Another interesting strategy of material combination was adopted to magnetically control the movement of scaffolds fabricated by 2pp. In this case, Ni/Ti bilayer was deposited on SU8 polymerized structures through e-beam evaporation of Ni and subsequent Ti deposition. Thanks to this approach it has been possible to obtain actual micro-devices, such as 3D cell culture transportation systems, exploitable even for *in vivo* applications.³⁸

Finally, the possibility to obtain nano-composite scaffolds by combining different nanomaterials with photoresists opens new perspectives for obtaining a huge variety of active/sensitive high resolution 3D structures. To date, examples of nanomaterials embedded in UV-curable materials used for the 3D fabrication by 2pp are represented by single-wall carbon nanotubes (SWCNTs), which have been aligned in the direction of the laser scanning,³⁹ titanium dioxide nanoparticles,⁴⁰ magnetic nanoparticles,⁴¹ and zinc oxide nanowires.⁴² The resulting composite material could theoretically allow for the mimicking of some physical features of the natural systems, such as conductivity and piezoelectricity, and so to contribute to resemble and/or mimic various physiological phenomena, including the activity of neuronal networks and of the cochlear sensory epithelium.

2pp structures for biological investigations

Cell/substrate interaction investigation

The control of the 3D microenvironment and of the surface topography thanks to 2pp technique allows an intense investigation of the cell-substrate biophysical interactions to be performed. The majority of biophysical studies made by taking advantage of 2pp have been focused on cell adhesion, shape, migration, proliferation, differentiation and function.

Recently, our group demonstrated 2pp fabrication (in Ormocomp®) of Brownian surfaces characterized by pre-determined Hurst exponent (H) and investigated the mesenchymal stem cell (MSC) cytoskeleton response to these substrates (Figure 1). In order to give a reliable mechanical support to the surfaces, we developed an innovative manufacturing strategy based on a line-by-line multilayer laser writing approach (Figure 1a). With this method, we obtained fractal surfaces characterized by $0.01 \leq H \leq 1.00$, and self-affine in the range of two spatial frequency decades (from 0.1 to 10 μm), a much wider range than that obtained with other chemical methods.⁶ Figure 1b shows the atomic force microscopy (AFM) characterization of the surfaces characterized by different H and the cytoskeleton of MSCs grown on these substrates. Interestingly, our findings revealed

Cite this: DOI: 10.1039/c0xx00000x

www.rsc.org/xxxxxx

MINIREVIEW

significant effects of fractality on stress fiber formation and, consequently, on cell adhesion and stiffness (in terms of E), coherently to the mechanical model based on the tensegrity architecture.⁷

Concerning the investigation of cell guidance owing to particular features of the substrate, our group demonstrated as the presence of sub-micrometric ridges obtained through single-line 2pp, biomimicking the topographical cues of pioneer axons, was able to guide and promote the axonal outgrowth of two different neural models, rat PC12 and human SH-SY5Y. In particular, enhanced effects on neurite alignment and length were reported by increasing the ridge frequency; furthermore, the presence of the patterned topographical cues on the 2pp fabricated substrates significantly enhanced the SH-SY5Y neural differentiation in terms of β 3-tubulin expression.⁴³ Another important study exploited 2pp for promoting NIH-3T3 fibroblast guidance. Interestingly, authors developed a technique for finely tuning the Ormocomp® ridge height by adjusting laser power, focus position and writing speed, and demonstrated that the fibroblast elongation was enhanced by increasing the ridge height, being the height threshold for obtaining fibroblast alignment of about 1 μ m.⁴⁴ The same group developed a fabrication method for 2pp of self-standing fibers between two glass plates and, after a fibronectin coating of the fibers, demonstrated the suitability of this 3D cell guidance system with NIH-3T3 fibroblasts and MDCK epithelial cell line.⁴⁵

Finally, 2pp technique has been adopted not only to investigate the interactions between substrates and eukaryotic cells, but also with prokaryotics. In this particular case, 3D structures have been used to control the bacterial growth (*E. coli*) and to investigate their trapping and migration.⁴⁶

Cell force measurement

2pp fabricated scaffolds are able to physically stimulate the cells, but, conversely, also cells can exert forces and elastically deform these structures: in particular, neurites and cardiomyocyte forces have been measured by exploiting 2pp structure deformability.^{34,43} The biophysical measurement of these forces is particularly important not only for the investigation of the cell-cell mechanical communication systems, but also for the analysis of their consequence on the mechanical properties and functions of the deriving tissues.⁴⁷ Concerning the cardiac tissue, cardiomyocytes were grown on a 3D cobweb-like structure based on pillars connected by beams, and the rhythmic contraction of the cells triggered the displacement of the elastic beams. The schemes of Figures 2a and 2b illustrate 2pp of the 3D network-like structure used for the cardiomyocyte force measurement. Figure 2c shows the scanning electron microscopy (SEM) image of the obtained 3D structure. In Figure 2d and 2e the oblique view and top view of the 3D confocal reconstruction of cardiomyocytes adhering to the 3D net-like structure are respectively reported. Taking

advantage of AFM measurement, Klein *et al.* were able to experimentally determine the displacement-force trend, thus evaluating the beam displacements triggered by a wide range of contraction forces.³⁴

Similarly, by fabricating sub-micrometric ridges for biomimicking the physical guidance of pioneer axons on developing neurites, our group reported as growing neural processes were able to bind and bend elastic ridge made with Ormocomp® with a force of about 3 nN, estimated through scanning ion conductance microscopy.⁴³ It is well known from the literature as this force intensities can be sustained by growing neurites, and are essential for the correct axonal elongation.⁴⁸

Cell migration

The proper modulation of cell migration is fundamental for many different physiological and/or pathological processes, including the correct development of the embryo, the regulation of the inflammatory response, and the formation of tumor metastasis.⁴⁹ In particular, the degree of cancer malignancy depends on the ability of the tumor cells to invade other tissues, also known as invasiveness.⁵⁰ The cells in the tissue can migrate in the 3D environment, guided by a multiplicity of chemical and physical cues, in extremely different conditions from those of standard 2D *in vitro* cultures. For this reason, the interest towards 3D biomimetic systems is enormously increased, being these models more easily accessible compared to *in vivo* models, and allowing high-throughput investigations on the mechanisms involved on cell migration to be performed.⁵¹

Taking advantage of 2pp technology, 3D matrix structures with modifiable pore sizes have been independently fabricated by several groups, and different mechanisms of cell migration were investigated. Tayalia *et al.* demonstrated that the 3D microenvironment promotes the enhancement of the cell speed compared to a 2D substrate. Furthermore, they were able to decrease the cell speed by decreasing the pore size of the 3D grid, so hindering the cell migration.⁵²

Instead, Olsen *et al.* investigated the dendritic cell migration by combining architectural and chemotactic components.⁵³ Thanks to a similar approach, Greiner *et al.* investigated the peculiar cell-type depending migration in the presence of a combination of different architectural-chemical-genetic factors.⁵⁴ In particular, they elegantly demonstrated as the mouse fibroblast cell invasion through a 3D pentaerythritol tetraacrylate (PETTA) grid was independent on the presence of chemotactic signals, but it could be significantly enhanced by reducing the nucleus stiffness through the knock-out of the lamin A/C gene. Conversely, epithelial A549 cell migration through little pores was promoted by chemoattractants, but appeared to be independent on the knock-out of lamin A/C, which also in this case induced a significant decrease of the nuclear stiffness. However, all the cell types were able to migrate more easily

Cite this: DOI: 10.1039/c0xx00000x

www.rsc.org/xxxxxx

MINIREVIEW

through the largest pores with respect to the little ones.

2pp for tissue engineering

The peculiar characteristics offered by 2pp technique (high resolution, repeatability and writing speed, which can be further increased by the use of galvanometric mirrors),⁵⁵ allow the preparation of series of 3D structures and/or extended patterned surfaces suitable for tissue engineering and regenerative medicine purposes.^{56,57} In particular, 2pp can be exploited both for the generation of well-defined topographical stimuli *in vitro* for the promotion of a specific tissue formation, on scaffolds that can be eventually re-implanted *in vivo*, and for the functionalization of implant surfaces with 3D architectures, in order to facilitate the integration of the biomedical devices in the tissues.

Concerning the *in vitro* topographical stimulation, it is well known from the literature as the micro/nanometric surface properties of a substrate can affect the cell proliferation/differentiation by acting on various mechanisms of mechanotransduction, often by altering the cell adhesion, the cytoskeletal conformation, the shape and the rigidity of the cell body, and the nucleus morphology.⁵⁸ Our group recently demonstrated as trabeculae-like structures bioinspired by μ -CT scans of human trabecular bone, and fabricated with 2pp of Ormocomp® thanks to a slice-by-slice approach (called "Osteoprints", Figure 3a) were able to reorganize the actin cytoskeleton, the cell adhesion, and the cell/nucleus shape, consequently strongly affecting the SaOS-2 bone-like cell proliferation and differentiation.²⁶ The presence of these 3D architectures, bioinspired by the shape of the fundamental units of the human trabecular bones, promoted the exit from the cell cycle both in presence and in absence of chemical factors, and strongly enhanced the *in vitro* osteogenic differentiation in terms of gene transcription and hydroxyapatite accumulation. Figure 3b is a pictorial representation obtained through the diagonal superposition of the μ -CT scan of a portion of the human trabecular bone, of a confocal acquisition of SaOS-2 osteoblast-like cells adhering to the Osteoprint, and of a further confocal acquisition of green-stained hydroxyapatite nodules accumulated in the SaOS-2 cultures.

In another work, rat MSCs were shown to *in vitro* invading and proliferating inside 3D cages prepared with the SZ2080 photoresist, mimicking the presence of stem cell niches (Figure 3c).⁵⁹ Differently from the observation carried out on our Osteoprints, rat MSCs populating 3D engineered niches were characterized by an increased percentage of Ki-67⁺ nuclei (Figure 3d), so demonstrating that the niche was able to maintain the stem cells in active proliferative conditions. The two different studies are not easily to compare because of the different material and of the different cell models adopted; however, it is possible to argue as the different 3D geometries play a key role in the control of proliferation vs. differentiation.

Indeed, while the stem cell niche architecture promotes a rounded morphology of the cell nucleus,⁶⁰ and thus a higher chromatin unfolding and a wider gene expression,⁶¹ the Osteoprints were conversely able to deform and compress the nuclei, thus promoting the exit from the cell cycle and enhancing the osteogenic differentiation.²⁶

Concerning the *in vitro* reconstruction of a particular tissue/system, endogenous vessel of different tissues, such as heart, cerebral cortex and retina, were 3D patterned by combining the architectural information of natural vessels, revealed through confocal microscopy, with the slice-by-slice 2pp of metalloproteinase-sensitive and fluorescently labeled poly(ethyleneglycol) hydrogels containing human umbilical vein endothelial cells (HUVECs) and 10T1/2 mesenchymal progenitors.²⁵ Embedded cells were organized in tubular structures inside the hydrogel, thus obtaining a faithful biomimetic vessel network just after 24 h of culture. Possible applications of this method are not limited to the regenerative medicine and to the field of biomaterials, but can also be considered for the *in vitro* modeling of pathological conditions, such as vascularization in presence of cancer and stroke.

Another interesting work reported on a bioinspired and high-quality reconstruction of a "compound eye", envisaging optical applications. The obtained hexagonal-shape "eye" was characterized by large numerical aperture ($NA = 0.4$), high fill factor ($FF = 100\%$), aspherical profile, and it was able to reduce imaging distortion by two/three times with respect to a single lens.⁶²

As previously mentioned, 2pp can be exploited for the surface modification with 3D structures for the promotion of the implant integration in the tissue. In the context of dental implant surface optimization, square patterns characterized by posts of 13 μ m height and 5 μ m diameter interconnected by rods were prepared.⁶³ More specifically, different distances (in the range 10 - 50 μ m) between posts were tested. Interestingly, authors demonstrated as a post distance of 10 μ m inhibits proliferation, while a 25 μ m spacing is able to promote the grown of osteoblast-like cells, thus suggesting a possible improved tissue/implant integration.

Other important approaches, exploiting both a multi-component polymer / protein combination⁶⁴ and the mineralization of the 3D structures through the "scaffold on scaffold" technique,⁶⁵ could allow for a more precise modulation of materials and architectures for an optimal implant surface modification.

Finally, medical devices of larger sizes can be fabricated through 2pp by using a combination of high laser power and low numerical aperture objectives, so increasing the size of the polymerization voxels. Thanks to this approach, large scale polymer scaffolds were fabricated for cardiovascular tissue engineering, and their biocompatibility was confirmed *in vivo*.⁶⁶ This technique could be also implemented with a multi-foci system based on hologram pattern technology, which allows the fabrication time to be strongly reduced.⁶⁷ Examples of

Cite this: DOI: 10.1039/c0xx00000x

www.rsc.org/xxxxxx

MINIREVIEW

millimetric-sized microstructured biomedical devices fabricated by 2pp are represented by microneedles,^{68,69} ossicular replacement prostheses,⁷⁰ and many other typologies of scaffolds.^{71,72}

Conclusions

Two-photon polymerization represents an innovative and flexible technology which allows the rapid prototyping of 3D structures for a wide range of biomedical applications, from millimetric-sized biomedical devices to nano-structured micrometric-sized surfaces for the investigation of cell/substrate interactions and for tissue engineering applications (Figure 4a). In Figure 4b, the histogram shows the temporal distribution of the publications on 2pp (blue bars) and on biological applications of 2pp (red bars). The rapid development of new photoresists and the combination of photocurable with other (nanostructured) materials could allow the generation of 3D structures characterized by a variety of active/sensitive and smart properties.

In the context of the biomimicking, taking advantage from ECM-like photoresists and owing to the 3D topographical reconstruction of *in vivo* tissue it is possible to recreate *in vitro* a natural-like micro/nano-environment for fostering different cell behaviors, including selective proliferation or differentiation, for the cell force and migration measurements, and for disease modeling. However, in order to move from *in vitro* models to the *in vivo* assessment of the developed scaffolds, the main issue is the production of large-enough 3D structures characterized, at the same time, by a high resolution. The enormous increase in terms of laser writing speed that can be achieved through the use of galvanometric mirrors⁵⁵ makes possible to dramatically improve the size of the structures, maintaining at the same time an optimal fabrication resolution. However, new technological up-grading are still necessary for a further increment of the technique performances, and, in particular, the high cost of 2pp systems is still a major obstacle for its wide-spread dissemination among the scientific community. Despite these drawbacks, we are fully confident that the tremendous potentialities of 2pp will soon make this technique a "golden standard" concerning micro- and nanofabrication, in particular in the biomedical field.

Figure captions

Figure 1. (a) The schematization illustrates the line-by-line multilayer fabrication method used for 2pp of fractal surfaces characterized by a pre-determined Hurst exponent (H). (b) In the first column, the 3D AFM rendering of surfaces characterized by $H = 1.00$, $H = 0.54$, $H = 0.01$; in the second column, immunofluorescence staining of mesenchymal stem cells (MSCs) grown on the different- H surfaces: f-actin in red, vinculin in green, nuclei in blue; in the third column, 3D

confocal reconstructions of MSCs on the different- H surfaces: f-actin in red, g-actin in green, nuclei in blue. Reproduced from [7] with permission by ACS.

Figure 2. (a) 2pp of a 3D network-like structure, obtained by exposingOrmocomp® photoresist to the laser. Model (b) and SEM image (c) of the obtained 3D structure. Tilted (d) and top (e) view of a 3D confocal reconstruction of cardiomyocytes adhering to the 3D structure, used for the cardiomyocyte contraction force measurements. Reproduced from [34] with permission by Wiley.

Figure 3. (a, b) The Osteoprint, a 3D bioinspired trabeculae-like structure fabricated by 2pp: (a) SEM scan of the Osteoprint; (b) diagonal superposition of three images representing, respectively, from top left to bottom right, the μ -CT 3D rendering of a portion of the human trabecular bone, the confocal acquisition of osteoblast-like cells adhering to the Osteoprint through focal adhesions (vinculin in green, f-actin in red, nuclei in blue), and the hydroxyapatite production during osteogenesis progression (hydroxyapatite in green and Osteoprint structure in red). (c, d) *In vitro* biomimicking of the stem cell niche. (c) SEM tilted image of the 2pp-engineered niche promoting stem cell homing: cells migrate into the niche and colonize its internal volume; (d) mesenchymal stem cells (MSCs) expressing the Ki-67 proliferation marker are mainly localized in the engineered niches. Reproduced from [26] and [59] with permission by Elsevier.

Figure 4. (a) Properties and applications of 2pp technology; in the center, a pictorial representation of the cytoskeleton of a cell adhering on a surface fabricated by 2pp (focal adhesions in green, f-actin in red and nucleus in blue). (b) Histogram showing the temporal progress of the number of publications on 2pp (blue bars) and on biological applications of 2pp (red bars).

Notes and references

^a Istituto Italiano di Tecnologia, Center for Micro-BioRobotics @SSSA, Viale Rinaldo Piaggio 34, 56025 Pontedera, Italy

^b Scuola Superiore Sant'Anna, The BioRobotics Institute, Viale Rinaldo Piaggio 34, 56025 Pontedera, Italy

* attilio.marino@iit.it; gianni.ciofani@iit.it

1. K. von der Mark, J. Park, S. Bauer and P. Schmuki, *Cell Tissue Res.*, 2010, **339**, 131–153.
2. P. Zorlutuna, N. Annabi, G. Camci-Unal, M. Nikkhah, J. M. Cha, J. W. Nichol, A. Manbachi, H. Bae, S. Chen and A. Khademhosseini, *Adv. Mater.*, 2012, **24**, 1782–1804.
3. S. C. Owen and M. S. Shoichet, *J. Biomed. Mater. Res. A*, 2010, **94A**, 1321–1331.
4. R. A. Gittens, T. McLachlan, R. Olivares-Navarrete, Y.

Cite this: DOI: 10.1039/c0xx00000x

www.rsc.org/xxxxxx

MINIREVIEW

- Cai, S. Berner, R. Tannenbaum, Z. Schwartz, K. H. Sandhage and B. D. Boyan, *Biomaterials*, 2011, **32**, 3395–3403.
5. F. Gentile, L. Tirinato, E. Battista, F. Causa, C. Liberale, E. M. di Fabrizio and P. Decuzzi, *Biomaterials*, 2010, **31**, 7205–7212.
6. F. Gentile, R. Medda, L. Cheng, E. Battista, P. E. Scopelliti, P. Milani, E. A. Cavalcanti-Adam and P. Decuzzi, *Sci. Rep.*, 2013, **3**.
7. A. Marino, A. Desii, M. Pellegrino, M. Pellegrini, C. Filippeschi, B. Mazzolai, V. Mattoli and G. Ciofani, *ACS Nano*, 2014, **8**, 11869–11882.
8. D. E. Discher, P. Janmey and Y.-L. Wang, *Science*, 2005, **310**, 1139–1143.
9. S. Nemir and J. L. West, *Ann. Biomed. Eng.*, 2010, **38**, 2–20.
10. S. Bodhak, S. Bose and A. Bandyopadhyay, *Acta Biomater.*, 2009, **5**, 2178–2188.
11. M. Padiál-Molina, P. Galindo-Moreno, J. E. Fernández-Barbero, F. O'Valle, A. B. Jódar-Reyes, J. L. Ortega-Vinuesa and P. J. Ramón-Torregrosa, *Acta Biomater.*, 2011, **7**, 771–778.
12. Y. Sun, K. M. A. Yong, L. G. Villa-Díaz, X. Zhang, W. Chen, R. Philson, S. Weng, H. Xu, P. H. Krebsbach and J. Fu, *Nat. Mater.*, 2014, **13**, 599–604.
13. M. L. Previtera, C. G. Langhammer and B. L. Firestein, *J. Biosci. Bioeng.*, 2010, **110**, 459–470.
14. C. A. Mullen, M. G. Haugh, M. B. Schaffler, R. J. Majeska and L. M. McNamara, *J. Mech. Behav. Biomed. Mater.*, 2013, **28**, 183–194.
15. A. J. Engler, M. A. Griffin, S. Sen, C. G. Bönnemann, H. L. Sweeney and D. E. Discher, *J. Cell Biol.*, 2004, **166**, 877–887.
16. A. Hertz and I. J. Bruce, *Nanomed.*, 2007, **2**, 899–918.
17. M. J. Dalby, N. Gadegaard, R. Tare, A. Andar, M. O. Riehle, P. Herzyk, C. D. W. Wilkinson and R. O. C. Oreffo, *Nat. Mater.*, 2007, **6**, 997–1003.
18. I. Tonazzini, E. Bystrenova, B. Chelli, P. Greco, P. Stoliar, A. Calò, A. Lazar, F. Borgatti, P. D'Angelo, C. Martini and F. Biscarini, *Biophys. J.*, 2010, **98**, 2804–2812.
19. S. Maruo, O. Nakamura and S. Kawata, *Opt. Lett.*, 1997, **22**, 132–134.
20. S. Reškštytė, M. Malinauskas and S. Juodkazis, *Opt. Express*, 2013, **21**, 17028–17041.
21. S. Juodkazis, V. Mizeikis, K. K. Seet, M. Miwa and H. Misawa, *Nanotechnology*, 2005, **16**, 846.
22. V. Ajeti, C.-H. Lien, S.-J. Chen, P.-J. Su, J. M. Squirrell, K. H. Molinarolo, G. E. Lyons, K. W. Eliceiri, B. M. Ogle and P. J. Campagnola, *Opt. Express*, 2013, **21**, 25346–25355.
23. B. H. Cumpston, S. P. Ananthavel, S. Barlow, D. L. Dyer, J. E. Ehrlich, L. L. Erskine, A. A. Heikal, S. M. Kuebler, I.-Y. S. Lee, D. McCord-Maughon, J. Qin, H. Röckel, M. Rumi, X.-L. Wu, S. R. Marder and J. W. Perry, *Nature*, 1999, **398**, 51–54.
24. W. Haske, V. W. Chen, J. M. Hales, W. Dong, S. Barlow, S. R. Marder and J. W. Perry, *Opt. Express*, 2007, **15**, 3426.
25. J. C. Culver, J. C. Hoffmann, R. A. Poché, J. H. Slater, J. L. West and M. E. Dickinson, *Adv. Mater.*, 2012, **24**, 2344–2348.
26. A. Marino, C. Filippeschi, G. G. Genchi, V. Mattoli, B. Mazzolai and G. Ciofani, *Acta Biomater.*, 2014.
27. Z. Ma, S. Koo, M. A. Finnegan, P. Loskill, N. Huebsch, N. C. Marks, B. R. Conklin, C. P. Grigoropoulos and K. E. Healy, *Biomaterials*, 2014, **35**, 1367–1377.
28. K.-S. Lee, R. H. Kim, D.-Y. Yang and S. H. Park, *Prog. Polym. Sci.*, 2008, **33**, 631–681.
29. E. Martínez, E. Engel, J. A. Planell and J. Samitier, *Ann. Anat.*, 2009, **191**, 126–135.
30. J. Torgersen, X.-H. Qin, Z. Li, A. Ovsianikov, R. Liska and J. Stampfl, *Adv. Funct. Mater.*, 2013, **23**, 4542–4554.
31. A. M. Kasko and D. Y. Wong, *Future Med. Chem.*, 2010, **2**, 1669–1680.
32. Š. Selimović, J. Oh, H. Bae, M. Dokmeci and A. Khademhosseini, *Polymers*, 2012, **4**, 1554–1579.
33. S.-H. Lee, J. J. Moon and J. L. West, *Biomaterials*, 2008, **29**, 2962–2968.
34. F. Klein, T. Striebel, J. Fischer, Z. Jiang, C. M. Franz, G. von Freymann, M. Wegener and M. Bastmeyer, *Adv. Mater.*, 2010, **22**, 868–871.
35. A. M. Greiner, B. Richter and M. Bastmeyer, *Macromol. Biosci.*, 2012, **12**, 1301–1314.
36. M. Farsari, M. Vamvakaki and B. N. Chichkov, *J. Opt.*, 2010, **12**, 124001.
37. F. Klein, B. Richter, T. Striebel, C. M. Franz, G. von Freymann, M. Wegener and M. Bastmeyer, *Adv. Mater.*, 2011, **23**, 1341–1345.
38. S. Kim, F. Qiu, S. Kim, A. Ghanbari, C. Moon, L. Zhang, B. J. Nelson and H. Choi, *Adv. Mater.*, 2013, **25**, 5863–5868.
39. S. Ushiba, S. Shoji, K. Masui, J. Kono and S. Kawata, *Adv. Mater.*, 2014, **26**, 5653–5657.
40. X.-M. Duan, H.-B. Sun, K. Kaneko and S. Kawata, *Thin Solid Films*, 2004, **453–454**, 518–521.
41. J. Wang, H. Xia, B.-B. Xu, L.-G. Niu, D. Wu, Q.-D. Chen and H.-B. Sun, *Opt. Lett.*, 2009, **34**, 581–583.
42. R. D. Fonseca, D. S. Correa, E. C. Paris, V. Tribuzi, A. Dev, T. Voss, P. H. B. Aoki, C. J. L. Constantino and C. R. Mendonca, *J. Polym. Sci. Part B Polym. Phys.*, 2014,

Cite this: DOI: 10.1039/c0xx00000x

www.rsc.org/xxxxxx

MINIREVIEW

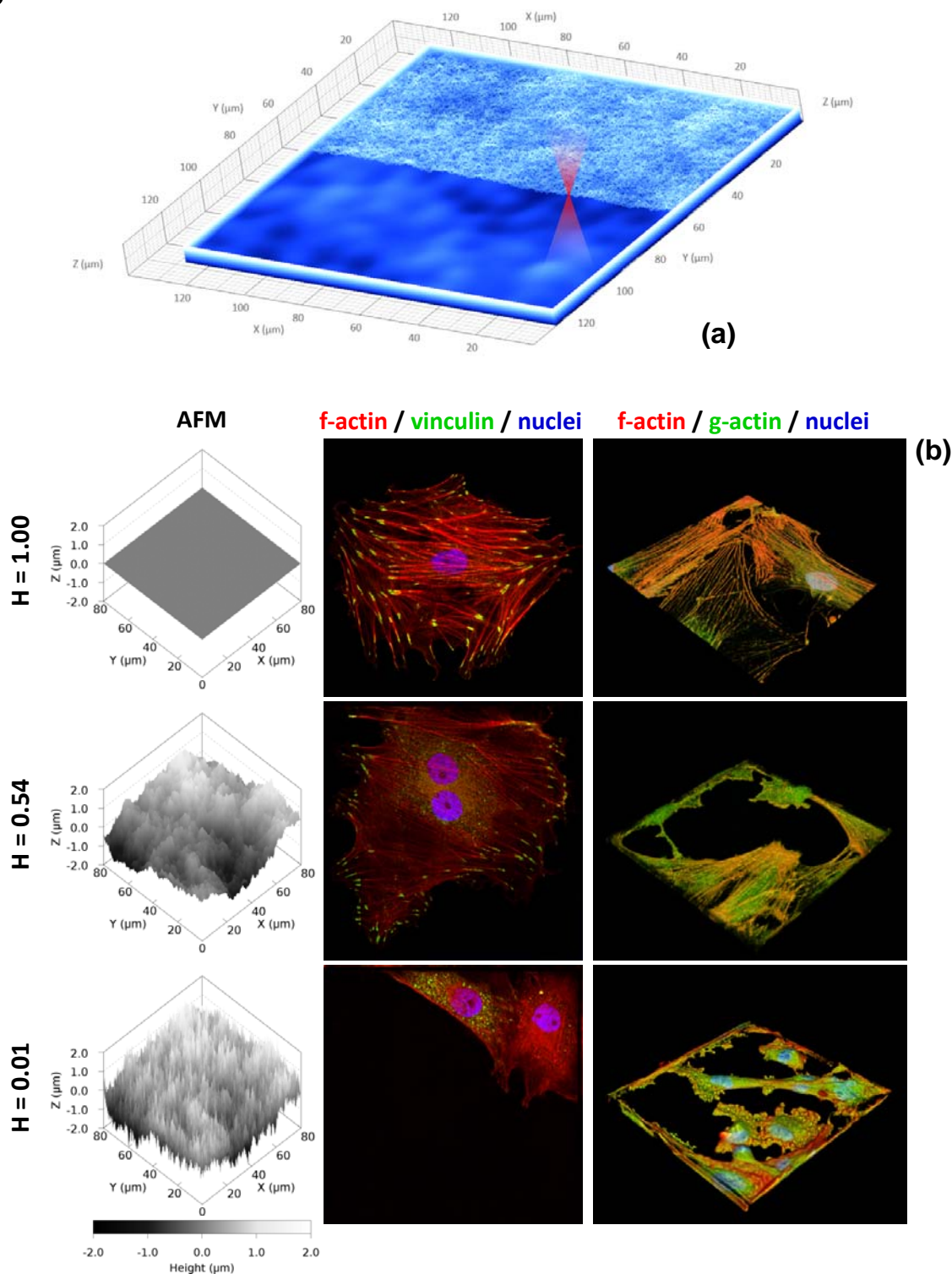
- 52, 333–337.
43. A. Marino, G. Ciofani, C. Filippeschi, M. Pellegrino, M. Pellegrini, P. Orsini, M. Pasqualetti, V. Mattoli and B. Mazzolai, *ACS Appl. Mater. Interfaces*, 2013, **5**, 13012–13021.
 44. H. Jeon, H. Hidai, D. J. Hwang and C. P. Grigoropoulos, *J. Biomed. Mater. Res. - Part A*, 2010, **93**, 56–66.
 45. H. Hidai, H. Jeon, D. J. Hwang and C. P. Grigoropoulos, *Biomed. Microdevices*, 2009, **11**, 643–652.
 46. A. J. G. Otuka, D. S. Corrêa, C. R. Fontana and C. R. Mendonça, *Mater. Sci. Eng. C Mater. Biol. Appl.*, 2014, **35**, 185–189.
 47. C. A. Reinhart-King, M. Dembo and D. A. Hammer, *Biophys. J.*, 2008, **95**, 6044–6051.
 48. S. R. Heidemann, P. Lamoureux and R. E. Buxbaum, *Cell Biochem. Biophys.*, 1997, **27**, 135–155.
 49. J. P. Thiery, H. Acloque, R. Y. J. Huang and M. A. Nieto, *Cell*, 2009, **139**, 871–890.
 50. M. Makale, *Birth Defects Res. Part C - Embryo Today Rev.*, 2007, **81**, 329–343.
 51. N. Kramer, A. Walzl, C. Unger, M. Rosner, G. Krupitza, M. Hengstschläger and H. Dolznig, *Mutat. Res.*, 2013, **752**, 10–24.
 52. P. Tayalia, C. R. Mendonca, T. Baldacchini, D. J. Mooney and E. Mazur, *Adv. Mater.*, 2008, **20**, 4494–4498.
 53. M. H. Olsen, G. M. Hjortø, M. Hansen, Ö. Met, I. M. Svane and N. B. Larsen, *Lab. Chip*, 2013, **13**, 4800–4809.
 54. A. M. Greiner, M. Jäckel, A. C. Scheiwe, D. R. Stamow, T. J. Autenrieth, J. Lahann, C. M. Franz and M. Bastmeyer, *Biomaterials*, 2014, **35**, 611–619.
 55. K. Obata, A. El-Tamer, L. Koch, U. Hinze and B. N. Chichkov, *Light Sci. Appl.*, 2013, **2**, e116.
 56. M. T. Raimondi, S. M. Eaton, M. M. Nava, M. Laganà, G. Cerullo and R. Osellame, *J. Appl. Biomater. Funct. Mater.*, 2012, **10**, 55–65.
 57. S. D. Gittard, A. Koroleva, A. K. Nguyen, E. Fadeeva, A. Gaidukeviciute, S. Schlie-Wolter, R. J. Narayan and B. Chichkov, *Front. Biosci. Elite Ed.*, 2013, **5**, 602–609.
 58. P. Tsimbouri, N. Gadegaard, K. Burgess, K. White, P. Reynolds, P. Herzyk, R. Oreffo and M. J. Dalby, *J. Cell. Biochem.*, 2014, **115**, 380–390.
 59. M. T. Raimondi, S. M. Eaton, M. Laganà, V. Aprile, M. M. Nava, G. Cerullo and R. Osellame, *Acta Biomater.*, 2013, **9**, 4579–4584.
 60. M. T. Raimondi, M. M. Nava, S. M. Eaton, A. Bernasconi, K. C. Vishnubhatla, G. Cerullo and R. Osellame, *Micromachines*, 2014, **5**, 341–358.
 61. M. Versaevel, T. Grevesse and S. Gabriele, *Nat. Commun.*, 2012, **3**.
 62. D. Wu, J.-N. Wang, L.-G. Niu, X. L. Zhang, S. Z. Wu, Q.-D. Chen, L. P. Lee and H. B. Sun, *Adv. Opt. Mater.*, 2014, **2**, 751–758.
 63. R. Wittig, E. Waller, G. von Freymann and R. Steiner, *J. Laser Appl.*, 2012, **24**, 042011.
 64. S. Reksityte, *J. Laser MicroNanoengineering*, 2014, **9**, 25–30.
 65. K. Terzaki, E. Kalloudi, E. Mossou, E. P. Mitchell, V. T. Forsyth, E. Rosseeva, P. Simon, M. Vamvakaki, M. Chatzinikolaidou, A. Mitraki and M. Farsari, *Biofabrication*, 2013, **5**, 045002.
 66. P. Danilevicius, S. Reksityte, E. Balciunas, A. Kraniauskas, R. Jarasiene, R. Sirmenis, D. Baltrikiene, V. Bukelskiene, R. Gadonas and M. Malinauskas, *J. Biomed. Opt.*, 2012, **17**, 081405–081401.
 67. S. D. Gittard, A. Nguyen, K. Obata, A. Koroleva, R. J. Narayan and B. N. Chichkov, *Biomed. Opt. Express*, 2011, **2**, 3167–3178.
 68. A. Doraiswamy, C. Jin, R. J. Narayan, P. Mageswaran, P. Mente, R. Modi, R. Auyeung, D. B. Chrisey, A. Ovsianikov and B. Chichkov, *Acta Biomater.*, 2006, **2**, 267–275.
 69. S. D. Gittard, A. Ovsianikov, B. N. Chichkov, A. Doraiswamy and R. J. Narayan, *Expert Opin. Drug Deliv.*, 2010, **7**, 513–533.
 70. A. Ovsianikov, B. Chichkov, O. Adunka, H. Pillsbury, A. Doraiswamy and R. J. Narayan, *Appl. Surf. Sci.*, 2007, **253**, 6603–6607.
 71. A. Ovsianikov, M. Malinauskas, S. Schlie, B. Chichkov, S. Gittard, R. Narayan, M. Löbner, K. Sternberg, K.-P. Schmitz and A. Haverich, *Acta Biomater.*, 2011, **7**, 967–974.
 72. T. M. Hsieh, C. W. B. Ng, K. Narayanan, A. C. A. Wan and J. Y. Ying, *Biomaterials*, 2010, **31**, 7648–7652.

Cite this: DOI: 10.1039/c0xx00000x

www.rsc.org/xxxxxx

MINIREVIEW

Figure 1

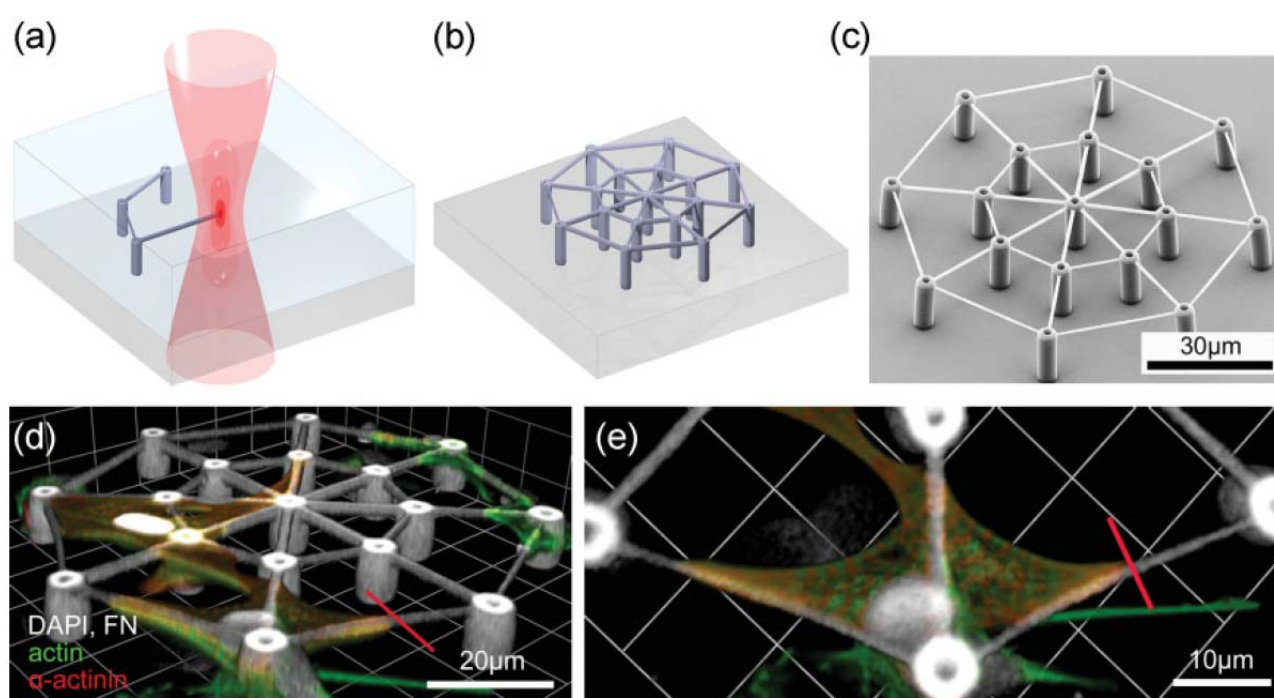


Cite this: DOI: 10.1039/c0xx00000x

www.rsc.org/xxxxxx

MINIREVIEW

Figure 2

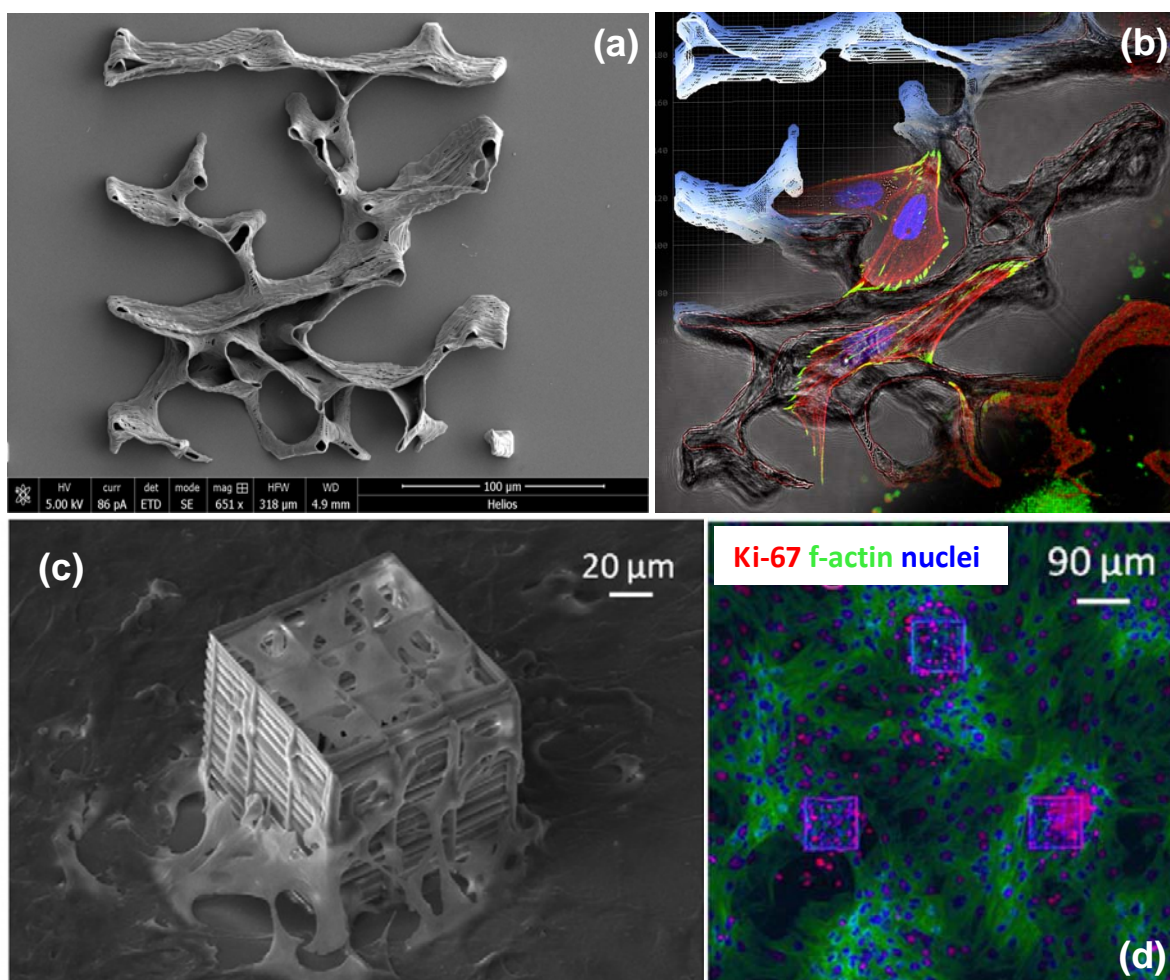


Cite this: DOI: 10.1039/c0xx00000x

www.rsc.org/xxxxxx

MINIREVIEW

Figure 3



Nanoscale Accepted Manuscript

Cite this: DOI: 10.1039/c0xx00000x

www.rsc.org/xxxxxx

MINIREVIEW

Figure 4

